UNIVERSITAT DE BARCELONA

Facultat de Matemàtiques
i Informàtica

GRAU DE MATEMÀTIQUES

Treball final de grau

THE SCHRÖDINGER EQUATION AND CHAOTIC DYNAMICS

Autor: Marta Botella Garcia

Director: Dr. Marina Gonchenko
Realitzat a: Departament de Matemàtiques i Informàtica

Barcelona, 13 de juny de 2022

Abstract

This work explores dynamical billiards and its general properties and focuses, in particular, in the Bunimovich stadium which is one of the most studied among known chaotic billiards. This project follows with the analytical resolution of the time independent Schrödinger equation for the case of the simple harmonic oscillator potential. It is also solved numerically for the one-dimensional and two-dimensional cases, developing a MATLAB programming that uses the finite-differences method with the aim to find the eigenvalues and eigenfunctions. Finally, the union of chaotic dynamics and quantum mechanics is explored to investigate quantum chaos and one of its most striking manifestations, quantum "'scars"'. The numerical analysis is able to replicate the evidence of scarring for the Bunimovich stadium.

2020 Mathematics Subject Classification. 34L40, 37C83, 65L15, 81Q05

Acknowledgements

I would like to express my deepest gratitude to my advisor Dr. Marina Gonchenko for her guidance, help and time invested. Her support and encouragement have been invaluable for the satisfactory completion of this work.

I also want to thank Agustí, Ikiru, Nausicaä, Nietzsche and Nuria for our particular chaotic dynamic.

Contents

Introduction

A large number of problems in Physics can be modelled as a billiard dynamical system: the building blocks are a point mass particle confined to a certain domain where it moves at constant speed and without friction and collides elastically with the billiard's boundary, whose geometry can be used to reproduce a broad variety of behaviours, including chaotic ones. It is the simplicity and pliability of the billiards that allow a plethora of issues in different disciplines to be analysed: from the behaviour of gas particles in a certain container, to optics, to a particle confined to an infinite square well.

Far from analytical and steady solutions, chaos is commonplace in most systems. There is yet no agreement in a definition of chaos, however, it perfectly evokes the persistent disorder and lack of regularity that a chaotic system has. This is why chaotic billiards are one of the most captivating types of billiards as well as most challenging, and one of the main elements in this thesis. Their study only dates back to the seventies, although some of them, such as the Bunimovich stadium, have been finely explored. Bunimovich introduced this billiard shaped as a rectangle capped by semicircles at each end and showed on [6] that such a surprisingly simple structure was ergodic and able to capture chaotic orbits as well.

Billiards are Hamiltonian systems and as such their state can be specified by the Hamilton-Jacobi equations with a certain associated potential V. Furthermore, the Hamiltonian formulation is considered a link between Classical Mechanics and Quantum Mechanics, which leads us to the next main element of this work.

Another popular and relatively recent discipline is Quantum Mechanics (QM). Its arrival brought with it the abandonment of the paradigm of classical physics, determinism. The formalism in itself became probabilistic: the theory unambiguously specifies the possible results of the experiment, but only provides their associated probabilities. Nevertheless, the fact that QM works with probabilities does

not mean that we lack some information about the system, but rather that the "'randomness"' is ingrained in the quantum approach.

One of the pinnacles of QM is the Schrödinger equation, $\hat{H}\psi = E\psi$, where $\hat{H}$ is the Hamiltonian operator of the quantum system. Its solutions provide the wave function, $\psi(\vec{r}, t)$ that describes the quantum state of our system at a particular point in time t. Its importance resides in the fact that the Schrödinger equation encapsulates the probabilistic character of QM, how the physical system evolves between measurements and the wave-particle duality.

When quantum mechanics and chaos coalesce, one gets quantum chaos and, in particular, chaotic quantum billiards. The study of the existence of chaos in quantum mechanics is a young field and, subsequently, a lot of questions remain unanswered. For the classically chaotic Bunimovich stadium, the determination of eigenvalues and eigenfunctions of the Schrödinger equation led to the discovery of some unexpected "'ridges"' when plotting the probability density of certain eigenvalues. These are symptoms of chaos in the classical framework that are manifested at the quantum level and are associated with unstable classical periodic orbits. In his paper [13], Heller called these regions of enhanced probability density quantum "'scars"'.

This work is organised as follows. Chapter 1 explores the dynamical system and properties of billiards and also introduces chaotic billiards, in particular, the Bunimovich stadium which will be the scenario where we will discuss quantum chaos and quantum "'scars"'. Chapter 2 dives into the Schrödinger equation. Analytical solutions are discussed for the particular case of the harmonic oscillator potential, also a numerical resolution is provided using the finite differences method for both one and two-dimensional cases. Ultimately, chapter 3 also uses a MATLAB code to numerically solve the Schrödinger equation in the Bunimovich stadium and computes the wave functions and eigenvalues in search of evidence of quantum chaos and quantum "'scars"'. Finally, the last section contains some concluding remarks and possible future directions on the topics here discussed.

Chapter 1

Billiards

1.1 Motivation

Mathematical billiards are models used to describe the inertial motion of a point mass in a frictionless domain Ω in which it freely moves at a constant velocity, continuously colliding with its boundary walls $\partial\Omega$ in a specular manner. That is, the billiard moves along a straight line, eventually bouncing off the boundary following the elastic reflection rule, namely, the angle of reflection equals the angle of incidence. Figure 1.1 shows how the point mass moves in a very simple setting, a circle billiard.

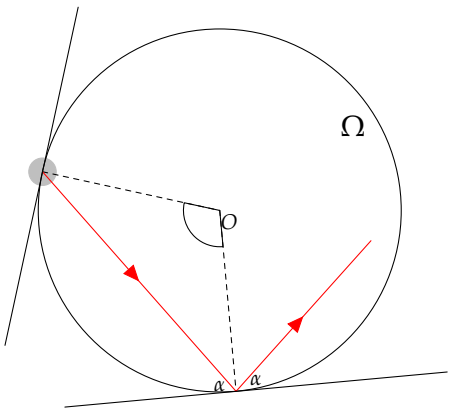

Figure 1.1: Billiard in a circle

Circle billiard tables have convex walls and as such have a focusing effect on the reflecting trajectories of the particle, as opposed to a dispersing effect.

The billiard trajectory is completely determined by the initial position, direction and velocity. Usually billiards appear when addressing many problems in classical mechanics. One of the most studied cases in classical thermodynamics corresponds to the Boltzmann gas whose particles are modelled as spheres that interact through elastic collisions among each other and with the container walls. The study of the mechanics of the gas particles can be reduced to a dynamical system of billiards.

As a general motivation, we will consider the example of a billiard in a square domain as seen in Figure 1.2. Let our domain be the unit square:

$$\Omega = \{(x, y) : 0 \leq x, y \leq 1\}.$$

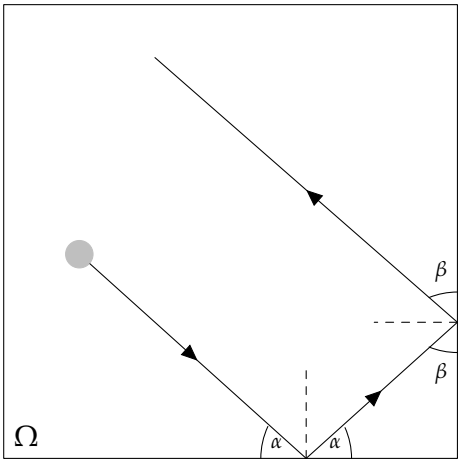

Figure 1.2: Billiard in a square

First, consider the trajectories that do not collide with the vertices of the square. As in [8] denote by $q_t = (x_t, y_t)$ the coordinates of the point mass at time t and by $v_t = (v_t^x, v_t^y)$ the velocity vector, where v_t^x and v_t^y correspond to the components of the velocity along the x and y axis, respectively. At a time $t + s$ and as long as the particle does not collide with the boundary, the laws of motion allow us to compute its position and velocity by the equations of a uniform rectilinear motion problem:

$$\begin{aligned} x_{t+s} &= x_t + v_t^x s \quad , \quad v_{t+s}^x = v_t^x \\ y_{t+s} &= y_t + v_t^y s \quad , \quad v_{t+s}^y = v_t^y \end{aligned} \tag{1.1}$$

When the particle collides with the boundary

$$\partial\Omega = \{\{0,1\} \times [0,1] \cup [0,1] \times \{0,1\}\},$$

the velocity vector v gets reflected across the tangent line to $\partial\Omega$ at the point of collision. As a result of the elastic collision, the normal component changes sign while the tangential component remains unchanged, that is, if the particle collides with a vertical side of the Ω region at time t, then $v_t^x = -v_t^x$ while v_t^y remains the same; on the other hand, if it strikes a horizontal side, then v_t^x is unchanged and $v_t^y = -v_t^y$. Consequently, the velocity norm does not change and the vector v can be assimilated to a unit vector. After $m \in \mathbb{Z}$ number of collisions with the vertical sides and $n \in \mathbb{Z}$ with the horizontal sides, the velocity of the particle will be

$$v_t^x = (-1)^m v_0^x \quad \text{and} \quad v_t^y = (-1)^n v_0^y \tag{1.2}$$

where v_0^x and v_0^y are the components along the x and y axis of the initial velocity.

After a reflection, the particle resumes again its free motion inside the domain Ω, until it collides again with the boundary and so on. Without any frictional or external forces, this type of motion can continue infinitely. Nonetheless, for a particle that collides against a vertex of the polygon, the reflection rule does not apply and its trajectory ends. This type of trajectories are called *singular*.

In this example, and as stated in [7], the orbit of the billiard is the set of broken lines in the configuration space that represent the free motion paths within the domain and the corresponding reflections off its boundary.

We can now look at the orbit of the billiard under a different light. Instead of reflecting its trajectory back to the interior of Ω after any strike to any of the sides, we reflect the polygon across the respective collision side. We can do this since the boundary of a polygon has smooth and flat components. As in [8], the replicas of Ω are denoted by

$$\Omega_{m,n} = \{(x,y) : m \leq x \leq m+1, n \leq y \leq n+1\}. \tag{1.3}$$

The set of these replicas $\Omega_{m,n}$ tiles the plane $\mathbb{R}^2$ as a square grid. As we can observe in Figure 1.3, the *unfolding* of the billiard trajectory yields a straight line on the plane. Therefore, periodic orbits in billiards in polygon tables are never isolated [7]. To recover the original trajectory in Ω, the reverse process is carried out, folding the successive adjacent created copies of Ω back onto themselves. Two lines in the plane correspond to the same billiard trajectory if they differ by a

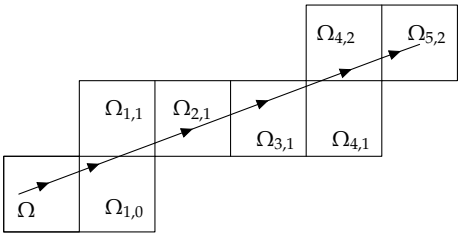

Figure 1.3: Unfolding of the billiard trajectory in a square [8]

translation through a vector from the lattice $2\mathbb{Z} + 2\mathbb{Z}$.

This method provides more information about the orbit of the billiard. For instance, if the slope of the trajectory is a rational number, $\frac{v_0^y}{v_0^x} \in \mathbb{Q}$, then the billiard trajectory is periodic; if it is irrational, $\frac{v_0^y}{v_0^x} \notin \mathbb{Q}$, then the trajectory is dense and uniformly distributed in the square.

As stated in [18], with this method we can further extract the number of periodic trajectories of a certain length L. If we consider a trajectory that goes from the origin to the point $(2p, 2q)$, its length equals $2\sqrt{p^2 + q^2}$. Thus, since the unfolding of a periodic trajectory is a segment in the plane whose end-points differ by a vector from the lattice $2\mathbb{Z} + 2\mathbb{Z}$, the number of periodic trajectories of length L is the number of pairs of integers that satisfy $p^2 + q^2 < L^2/2$.

Starting from the tiled $\mathbb{R}^2$ plane by the squares $\Omega_{m,n}$, consider the set of four unit squares that have one common vertex

$$\mathbb{K}_2 = \{(x, y) : 0 \leq x, y \leq 2\}.$$

Observe that the parallel translations of $\mathbb{K}_2$ also cover the entire plane. Therefore, identifying the opposite sides of $\mathbb{K}_2$, we are able to construct a torus where we can study the unfolded trajectories as geodesics.

It is worth noting that billiards in polygons are non-chaotic [7], in the sense that if the sequence of sides where the particle has collided is known, then the future sequence of sides from which it will be reflected is uniquely defined.

1.2 Fundamentals

After an intuitive explanation of billiards, this section introduces the fundamentals of the theory behind them. Note that we will restrict our study to two-

dimensional billiards.

A billiard in a planar region is defined as follows:

Definition 1.1. *Let $\Omega \subset \mathbb{R}^2$ be a bounded connected domain with a piece-wise smooth boundary $\partial\Omega$. A billiard system represents the free motion of a point particle inside the Ω region with elastic reflections off the boundary.*

An important aspect of the billiard trajectory is the angle of incidence, which will be characterised as follows:

Definition 1.2. *The angle of incidence is the angle measured between the incoming trajectory and the line tangent to the boundary, at the point of collision.*

Following [8], the boundary of $\partial\Omega$ is a finite union of compact curves:

$$\partial\Omega = \Gamma_1 \cup \ldots \cup \Gamma_r. \tag{1.4}$$

Each curve Γ_i is defined by a continuous one-to-one C^2 map $f_i : [a_i, b_i] \to \mathbb{R}^2$. If $f_i(a_i) \neq f_i(b_i)$, then Γ_i is an arc; if $f_i(a_i) = f_i(b_i)$, then Γ_i is called a closed curve. We also assume that the boundary components Γ_i satisfy

$$\Gamma_i \cap \Gamma_j \subset \partial\Gamma_i \cup \partial\Gamma_j \quad i \neq j, \tag{1.5}$$

that is, the boundary elements can intersect each other only at their endpoints. Furthermore, the second derivative f_i'' can only either be $f_i'' \equiv 0$ or $f_i'' \neq 0$, in all $[a_i, b_i]$. According to the value of f_i'', billiard walls can be one of three types: **flat walls** when $f_i'' \equiv 0$; **focusing walls** if it is convex such as the circle introduced in the previous chapter; and **dispersing walls** when it is concave.

Since we have discussed a square billiard table in the previous section, we can define what is understood as polygon billiard:

Definition 1.3. *A polygonal billiard consists of a closed region Ω bounded by a convex polygon $\partial\Omega$ in the Euclidean plane $\mathbb{R}^2$ where a point mass moves, given initial position and direction.*

To construct the dynamics of the billiard, we follow the notation in the previous section and in [8]. Let $q(t) \in \Omega$ denote the position of the particle and $v(t) \in \mathbb{R}^2$ its velocity, as functions of time $t \in \mathbb{R}$. When the particle moves freely in the interior of the domain, $q \in \Omega^o$, its velocity remains constant and, hence, follows:

$$\dot{q} = v \qquad \dot{v} = 0 \tag{1.6}$$

When the particle collides with the boundary of the domain, $q \in \partial\Omega$, its velocity changes instantaneously and it is reflected across the tangent to $\partial\Omega$ at the point of collision q. This stems from the rule that the angle of incidence is equal to the angle of reflection and, thus, establishes the following relation between the velocity vectors before v^- and after v^+ the collision

$$v^+ = v^- - 2\langle v, n\rangle n, \tag{1.7}$$

where n is the unit normal vector to $\partial\Omega$. Equations (1.6) and (1.7) describe the laws of motion of the billiard and preserve the norm of the velocity vector v which is then taken to be equal to the unit. Henceforth we will consider the vector v to be the direction vector which, for every $p \in \partial\Omega$, will define an angle with the tangent vector to $\partial\Omega$, measured counter-clockwise.

If the moving billiard collides with a vertex of the domain Ω, its trajectory stops. Otherwise, the trajectory of the particle is defined at all times $-\infty < t < \infty$ by $(q(t), v(t))$, where $q \in \Omega$ and $v \in S^1$.

Definition 1.4. *A collision is regular if the billiard strikes the boundary at a regular smooth component Γ_i for some i and the velocity vector v^- is not tangent to $\partial\Omega$.*

As we have introduced, the state of the particle at a time t is determined by the pair $(q(t), v(t))$ where $q \in \Omega$ and $v \in S^1$. With this, we can define the phase space of the system.

Definition 1.5. *The phase space of the dynamical system of the billiard is*

$$\Lambda = \{(q, v)\} = \Omega \times S^1. \tag{1.8}$$

It is a three-dimensional manifold with boundary $\partial\Lambda = \partial\Omega \times S^1$.

Now, let M be the unit tangent vector space of $x = (q, v)$ such that $q \in \partial\Omega$. Consider $x = (q, v)$ the initial vector of the billiard ball and $x' = (q', v')$ the vector when the billiard collides with the boundary at point q' with reflected velocity v'. Then we define the following application:

Definition 1.6. *The billiard ball map*

$$\begin{aligned} T : M &\to M \\ (q, v) &\to (q', v') \end{aligned} \tag{1.9}$$

Now, we have the elements to define the billiard orbit:

Definition 1.7. *A billiard orbit is the set of pairs (q, v) that generate a billiard trajectory. It is obtained from the segmented paths drawn by the billiard through its free motion within Ω and the vertices corresponding to the collisions off the boundary following a direction determined by the reflection rule.*

In other words, given an initial point x_0, the dynamical system T evolves with each iteration following $x_1 = T(x_0), x_2 = T^2(x_0), \ldots, x_n = T^n(x_0), \ldots$. The sequence $\mathcal{O}(x_0) = \{x_0, x_1, x_2, \ldots, x_n, \ldots\}$ is the orbit of the system associated to starting condition x_0. In the context of billiards, an orbit will be the ordered sequence of collision points with the boundary of the billiard table, each point having associated the a position−direction, (q, v), in the phase space Λ.

An interesting type of orbit are periodic orbits:

Definition 1.8. *A periodic orbit is an orbit in which the billiard ball returns to its initial position with the same initial angle.*

Therefore, a periodic orbit is a type of solution of the dynamical system that repeats itself as time evolves. In our initial example of a billiard in a square table, a periodic orbit is encountered when the billiard strikes the boundary at an angle equal to $\pi/2$. If the billiard strikes at point A perpendicular to the boundary, it will move to point B and, without friction, it will move between these points infinitely, as shown in Figure 1.4. The points A and B are known as *periodic points*.

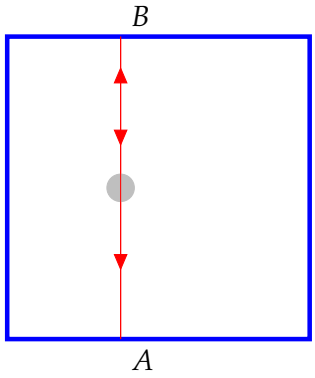

Figure 1.4: Periodic orbit of a billiard in a square

As stated in [7], billiard models are Hamiltonian systems with a potential V defined by:

$$V(q) = \begin{cases} 0 & \text{, if } q \in \Omega \\ \infty & \text{, if } q \in \partial\Omega \end{cases}$$

Because the dynamics of billiards are defined by the shape of their boundary, they enable the replication of a large variety of possible behaviours of Hamiltonian systems from regular to completely chaotic ones. If the Hamiltonian system is conservative, then the billiard also satisfies the energy and momentum conservation laws.

Billiards have been largely studied in connection to ergodic theory. To arrive at the ergodicity of a dynamical system first we need to acquaint ourselves with measure theory.

Definition 1.9. *[8] Let X be a set and $\mathcal{F}$ a $\sigma-$algebra on X. A measure μ on $(X, \mathcal{F})$ is a function $\mu : \mathcal{F} \to \mathbb{R} \cup \{+\infty\}$ that satisfies the following properties:*

- *non-negativity: $\mu(A) \geq 0$ for all $A \in \mathcal{F}$*
- *null empty set: $\mu(\emptyset) = 0$*
- *countable additivity: if $\{A_i\}_{i=1}^{\infty} \in \mathcal{F}$ and $A_i \cap A_j = \emptyset$ for $i \neq j$, then $\mu\left(\cup_{i=1}^{\infty} A_i\right) = \sum_{i=1}^{\infty} \mu(A_i)$*

$(X, \mathcal{F})$ is called a measurable space.

If we require that a measure μ return values in the unit interval $[0, 1]$ such that $\mu(X) = 1$ and $\mu(\emptyset) = 0$, then it is called a **probability measure**.

Let $(X, \mathcal{F})$ be a measurable space and T a transformation $T : X \to X$.

Definition 1.10. *We say that T is a measurable transformation if $T^{-1}(A) \in \mathcal{F}$ for every $A \in \mathcal{F}$.*

Definition 1.11. *A measurable transformation T preserves the measure μ if for all $A \in \mathcal{F}$, $\mu(T^{-1}(A)) = \mu(A)$. We can also say that μ is $T-$invariant.*

These elements conform a measure-preserving dynamical system $(X, \mathcal{F}, \mu, T)$. Finally, we are equipped to provide a formal definition of ergodicity.

Definition 1.12. *Let $(X, \mathcal{F})$ be a measurable space and μ a probability measure on $(X, \mathcal{F})$. Consider $T : X \to X$ a measurable transformation. We say that T is $\mu-$ergodic if:*

- *T preserves μ, and*
- *for any $A \in \mathcal{F}$ such that $T^{-1}(A) \subset A$, either $\mu(A) = 0$ or $\mu(A) = 1$.*

That is, a dynamical system is ergodic if all its invariant subsets are non-trivial.

In the context of billiards [18], ergodicity means that, given any initial condition, the consecutive iterations of the billiard ball map T will completely cover the phase space and that the only subsets that are invariant under T will have either zero or full measure.

Billiards in rational polygons[1] are non-ergodic because there is a finite number of possible directions for their orbits. However, a billiard in a typical polygon is ergodic. Nevertheless, all these billiards are non-chaotic, since all their boundary components are flat.

1.3 Chaotic billiards

It has been observed that most billiards show a chaotic behaviour. This means that dynamical billiards are characterised by uncertainty in their motion and a high sensitivity to initial conditions. Therefore, slight changes in the initial position or direction lead to large future deviations. This fact primarily stems from the characteristics of the boundary components.

Although there are many possible definitions of chaos and, scientifically, there is no agreement on it, we will follow the interpretation from [9]. According to Devaney, a chaotic dynamical system is characterised by three properties, namely, sensitivity to initial conditions, dense periodic orbits and transitivity. We will now briefly analysed each of these requisites.

Definition 1.13. *A dynamical system F is sensitive to initial conditions if there exists $\beta > 0$ such that for any initial condition x and any $\varepsilon > 0$, there exists $y \in \mathcal{B}_\varepsilon(x)$ and an iteration k such that $|F^k(x) - F^k(y)| \geq \beta$. Usually β grows exponentially with time, $\beta \sim \exp(t)$.*

Sensitive dependence on initial conditions is an important phenomenon in scientific research, as a result small initial differences originating from noise or round-offs are continuously magnified and can dramatically change the solution of the system.

The second property that a dynamical system has to satisfy to qualify as chaotic is that the set of periodic points must be dense in the phase space Λ. Following

[1] A polygon is rational if all its angles are rational multiples of π.

[16], this means that, any point $p \in \Lambda$ is either a periodic point or there is a periodic point sufficiently close to it. Formally,

Definition 1.14. *Given any point $p \in \Lambda$ and $\varepsilon > 0$, the set of periodic points is dense in Λ if there exists a periodic point $q_\varepsilon \in \Lambda$ such that $|p - q_\varepsilon| < \varepsilon$.*

The third and final concept involved in a chaotic dynamical system is transitivity:

Definition 1.15. *A dynamical system is transitive if for any points $x, y \in \Lambda$ and any $\varepsilon > 0$, there exists $z \in \mathcal{B}_\varepsilon(x)$ whose orbit includes points of $\mathcal{B}_\varepsilon(y)$.*

That is (as stated in [9]), given any two points of the dynamical system, this will be transitive if there exists an orbit that passes arbitrarily close to both. A dynamical system whose periodic points are dense is transitive. The converse is also true.

Finally, we can synthesise the definition of chaos as follows:

Definition 1.16. *A dynamical system is chaotic if:*

- *it is sensitive to initial conditions*
- *its periodic points are dense*
- *it is transitive*

The Bunimovich stadium billiard is one of the most famous mathematical objects in the research of dynamical systems and has been studied as a paradigm for chaotic billiards since it was introduced by Bunimovich in the mid-70s, [6]. A Bunimovich stadium is a rectangle capped by semi-circles at each end, as shown in Figure. 1.5. Its boundary is the union of the four components $\partial\Omega = \Gamma_1 \cup \Gamma_2 \cup \Gamma_3 \cup \Gamma_4$.

Both Γ_1 and Γ_3 are convex to the interior of the stadium, thus are called focusing; while both Γ_2 and Γ_4 are flat since they correspond to line segments. Therefore, the boundary amounts to a differentiable curve but with a discontinuous curvature at the points where Γ_1 and Γ_2 meet the arched components Γ_3 and Γ_4. Inside the boundary, we assume that there is no friction, so the billiard moves freely in straight paths with a constant velocity, meaning that its norm remains unchanged. When the billiard collides with the boundary, it bounces off with an angle equal to the angle of incidence.

As stated in [16] and mentioned in the previous section the phase space of the Bunimovich stadium dynamical system is the set of all ordered pairs (q, v) where

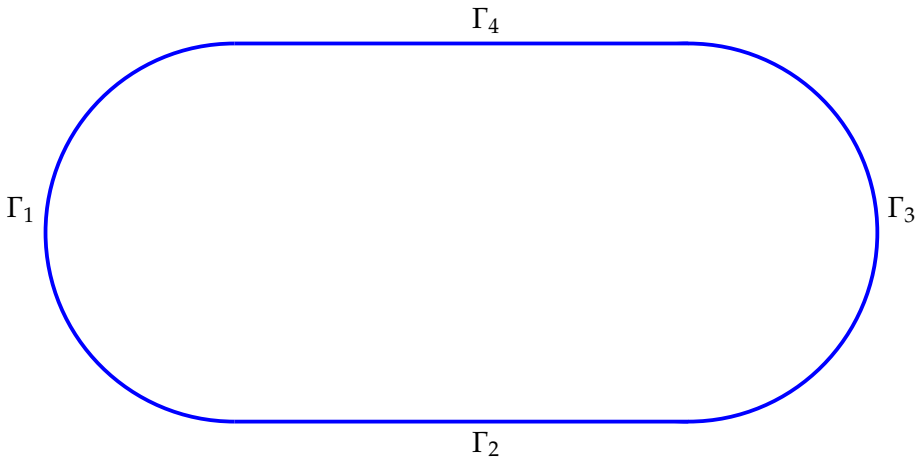

Figure 1.5: Bunimovich stadium

the first coordinate, q, refers to the position of the billiard within the billiard table and where we have taken the second coordinate to be the direction of the billiard, v, since its speed remains unchanged.

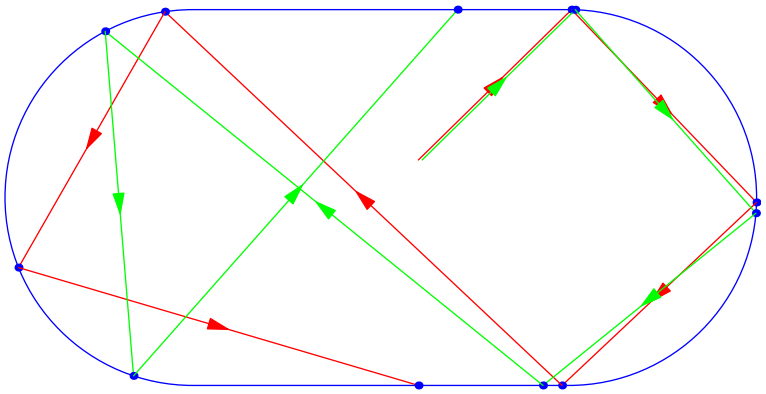

Figure 1.6: Sensitivity dependence to initial conditions in the Bunimovich stadium

Theorem 1.17. *[6] The Bunimovich stadium billiard is chaotic.*

The chaos in the Bunimovich dynamical system arises from the rectangular components of the boundary that counteract the focusing effect of the rounded convex semicircle ends. Figure 1.6 shows the trajectories of two billiards that initially move in the same direction although from slightly different positions. After each collision with the boundary of the stadium, the trajectories diverge and end up being very different only after six iterations. Therefore, the Bunimovich

stadium satisfies the first condition in definition 1.16 and shows dependency to starting conditions.

It also satisfies the second requisite of the definition of chaos 1.16. As in [16], we take any point in the boundary of the Bunivomich stadium, such as the point P in Figure 1.7, with an arbitrary direction. In a neighbourhood of P, there exists a point such as Q that is periodic, hence satisfying the second requirement.

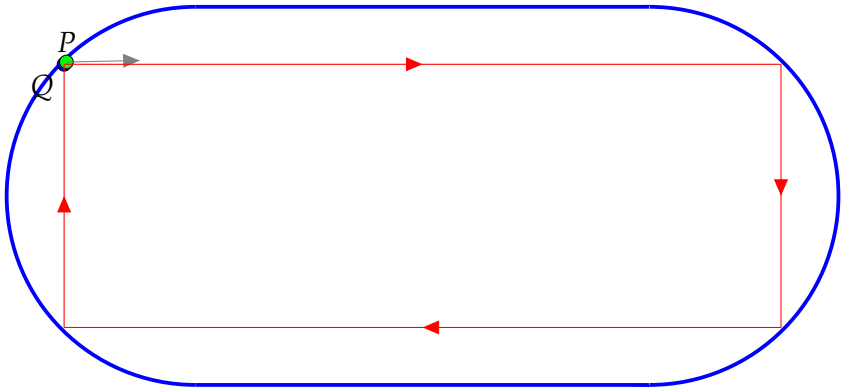

Figure 1.7: Set of periodic points in the Bunimovich stadium is dense

Finally we see that the Bunimovich stadium satisfies the transitivity property, following [16]. Let's consider, in Figure 1.8, two points $x, y \in \Lambda$ that correspond to the collision points AB and CD, respectively, that is, the first point x starts at point A and collides at point B while the second point y starts at point C and ends at D.

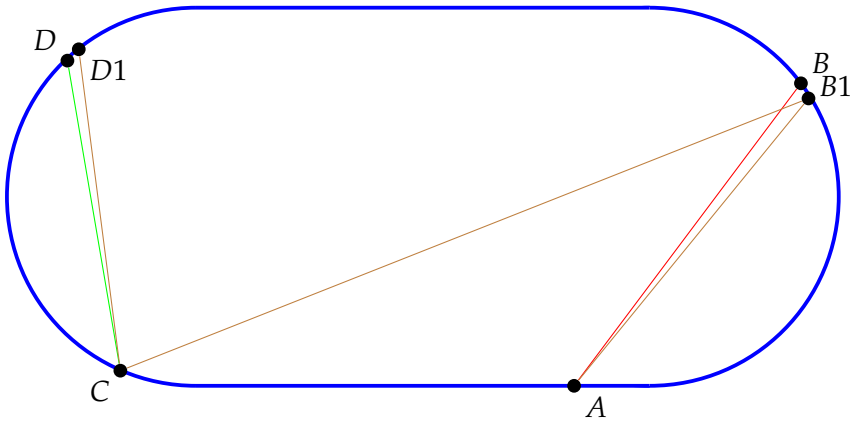

Figure 1.8: The Bunimovich stadium is transitive

According to the definition of transitivity, there must exist a third point $z \in \Lambda$ whose orbit passes arbitrarily close to x and y. We see diagrammatically that there exists a billiard that starts at A and collides with point $B1$ at the boundary of the stadium that subsequently collides with C and finally strikes again at $D1$. Thus, choosing as the third point $z = AB1$, we can see that its orbit satisfies the property of transitivity.

Finally, an important property of the Bunimovich stadium is that it constitutes an ergodic dynamical system, that is, given an starting point, x_0, its orbit $\mathcal{O}(x_0)$ tends to eventually contain all points (q, v) of the phase space. This can be seen also as a manifestation of chaos.

Theorem 1.18. *[6] The Bunimovich stadium billiard is ergodic.*

As can be seen in Figure 1.9, after only 100 iterations, the orbit of a billiard in the Bunimovich stadium passes through a large number of point-pairs (q, v) of the phase space.

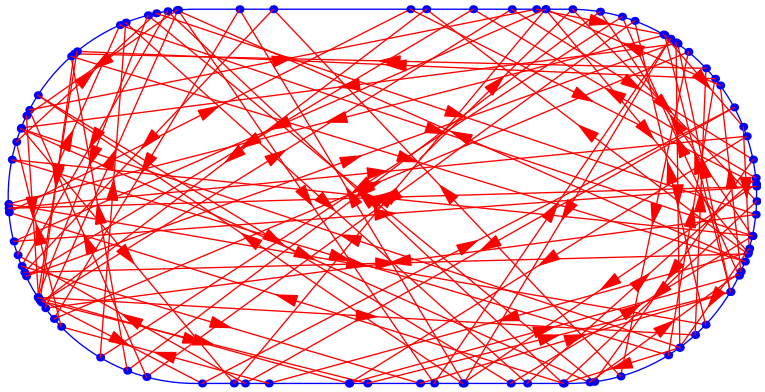

Figure 1.9: The Bunimovich stadium after 100 iterations

After 500 iterations, it is shown in Figure 1.10 that almost all the phase space associated to the Bunimovich stadium is covered and the billiard trajectory is almost uniformly distributed over the table.

Note that the set of non-ergodic (periodic) orbits has a zero measure.

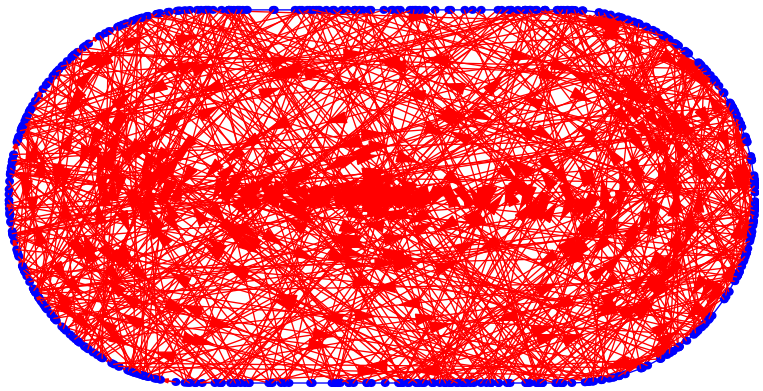

Figure 1.10: The Bunimovich stadium after 500 iterations

Chapter 2

The Schrödinger equation

Classical mechanics is governed by determinism. It is possible to establish a set of differential equations satisfying classical laws whose solution, given starting conditions, dictates a deterministic evolution of the system under study. However, several phenomena such as the photoelectric effect, the black-body radiation or the Compton radiation discovered at the beginning of the twentieth century challenged the laws of classical mechanics which ultimately showed themselves insufficient to explain these experiments. From Planck's theory of electromagnetic radiation by which energy is emitted and absorbed in discrete packets, called quanta,[1] to 1924, when De Broglie postulated that the wave-particle duality was applicable to all particles and, in general, to any body in motion, all these theories prompted the search for a procedure to describe the behaviour of any system of particles. The formalism in which it resulted is what is known as Quantum Mechanics (QM).

The basic essence of QM is the (time-dependent) Schrödinger equation, eq. (2.1), which is the wave equation whose solution corresponds to the wave function $\Psi(\vec{r}, t)$ that governs the behaviour of a quantum physical system:

$$i\hbar \frac{\partial \Psi}{\partial t}(\vec{r}, t) = \hat{H}\Psi(\vec{r}, t) \tag{2.1}$$

where $\hbar$ is Planck's constant, $\Psi(\vec{r}, t)$ is the wave function which depends on spatial coordinates $\vec{r}$ and time t, and $\hat{H}$ is the Hamiltonian operator of the system, yet to be quantified.

Unlike classical mechanics, it is not possible to determine both the position, $\vec{r}$ and momentum, $\vec{p}$, of a particle simultaneously due to Heisenberg's uncertainty

[1] The energy of a quantum is given by: $E = h\omega$, where ω is the frequency of radiation

principle. Therefore the state of a particle is described by a wave function whose interpretation under Schrödinger's theory is a probability density: despite the possible results of an experiment being unambiguously known, this formalism only provides the probability of these results. It is a generalization of Newton's second law that includes Newton's theory as a particular case in the classical limit.

The total energy of a non-relativistic particle is given by

$$E = \frac{p^2}{2m} + V(\vec{r}, t), \tag{2.2}$$

where m is the mass of the particle. The first term corresponds to the kinetic energy of the particle and V is the potential energy acting on the particle.

Rewriting equation (2.2) in terms of the canonical substitution $\vec{p} \leftrightarrow -i\hbar\vec{\nabla}$ (being $\vec{\nabla}$ the nabla operator) and $E \leftrightarrow i\hbar\frac{\partial}{\partial t}$, we recover the time-dependent Schrödinger equation and the Hamiltonian operator corresponds to the expression

$$\hat{H} = -\frac{\hbar^2}{2m}\nabla^2 + V(\vec{r}, t), \tag{2.3}$$

where ∇^2 is the Laplacian operator. This makes clear that the Hamiltonian operator corresponds to the total energy of the system. Assuming that the potential $V(\vec{r})$ does not depend on time, then the Hamiltonian in the Schrödinger equation is also time independent and the equation can be solved by separation of variables. Solutions will be the product of separate functions in $\vec{r}$ and t:

$$\Psi(\vec{r}, t) = \psi(\vec{r})f(t) \tag{2.4}$$

Substituting this previous expression in the time-dependent Schrödinger equation, we get

$$i\hbar\psi(\vec{r})\frac{df(t)}{dt} = \left[-\frac{\hbar^2}{2m}\nabla^2\psi(\vec{r}) + V(\vec{r})\psi(\vec{r})\right] f(t) \tag{2.5}$$

Dividing by ψf, the equation reads:

$$i\hbar\frac{1}{f(t)}\frac{df}{dt} = \frac{1}{\psi(\vec{r})}\left[-\frac{\hbar^2}{2m}\nabla^2\psi(\vec{r}) + V(\vec{r})\psi(\vec{r})\right] \tag{2.6}$$

For this equation to be true, both sides have to be equal to a constant value, which must have units of energy, so it is conveniently denoted by E. Thus, the

time-dependent Schrödinger equation can be separated into two ordinary differential equations:

$$\begin{cases} i\hbar\dfrac{df(t)}{dt} = Ef(t) \\ \left[-\dfrac{\hbar^2}{2m}\nabla^2 + V(\vec{r})\right]\psi(\vec{r}) = E\psi(\vec{r}) \end{cases} \tag{2.7}$$

The first of these equations can be immediately solved to get

$$f(t) = e^{-iEt/\hbar}. \tag{2.8}$$

The second equation is known as the **time-independent Schrödinger equation**:

$$\left[-\frac{\hbar^2}{2m}\nabla^2 + V(\vec{r})\right]\psi(\vec{r}) = E\psi(\vec{r}) \tag{2.9}$$

In a more compact way, equation (2.9) can be rewritten as

$$\hat{H}\psi_n(\vec{r}) = E_n\psi_n(\vec{r}) \tag{2.10}$$

which is the equation of eigenvalues for the Hamiltonian operator. This result also proves that the chosen separation constant E is, in fact, the total energy of the physical system.

Therefore, the formal solution of the time-dependent Schrödinger equation is a wave function of the form:

$$\Psi(\vec{r},t) = \psi(\vec{r})e^{-iEt/\hbar} \tag{2.11}$$

These solutions represent stationary states of the system since the probability density does not depend on time

$$|\Psi(\vec{r},t)|^2 = \psi^* e^{iEt/\hbar}\psi e^{-iEt/\hbar} = |\psi(\vec{r})|^2 \tag{2.12}$$

and are also states of definite total energy. The time-independent Schrödinger equation, eq.(2.9), leads to energy quantization: only the values of E whose eigenfunction $\psi(\vec{r})$ is solution of $\hat{H}\psi = E\psi$ are allowed. The eigenvalues of the Hamiltonian operator correspond to possible values of the spectrum of total energy.

Consequently, the general solution of the time-dependent Schrödinger equation can be written as a linear combination of stationary states of the form

$$\Psi(\vec{r},t) = \sum_{n=1}^{\infty} c_n\psi_n(\vec{r})e^{-iEt/\hbar} \tag{2.13}$$

To go any further with the Schrödinger equation, one has to specify a potential $V(\vec{r})$. One of the paradigms amongst potential energy functions in Physics is that of the harmonic oscillator

$$V(r) = \frac{1}{2}kr^2 \tag{2.14}$$

where $k = m\omega^2$ is the force constant and ω its angular frequency. It is important because it describes the behaviour of a great variety of physical systems and it is also able to approximate almost any potential in the neighbourhood of a local minimum.

For this particular potential, the time-independent Schrödinger equation becomes

$$-\frac{\hbar^2}{2m}\nabla^2\psi(\vec{r}) + \frac{1}{2}kr^2\psi(\vec{r}) = E\psi(\vec{r}) \tag{2.15}$$

In the next sections of this chapter, we will analyse the solution to equation (2.15) in one and two dimensions.

2.1 1D harmonic oscillator

The time-independent Schrödinger equation for the unidimensional harmonic oscillator takes the following form:

$$-\frac{\hbar^2}{2m}\frac{d^2\psi(x)}{dx^2} + \frac{1}{2}kx^2\psi(x) = E\psi(x). \tag{2.16}$$

To solve this equation, firstly, we make it dimensionless dividing by $\hbar\omega$:

$$-\frac{\hbar}{2m\omega}\frac{d^2\psi(x)}{dx^2} + \frac{m\omega}{2\hbar}x^2\psi(x) = \frac{E}{\hbar\omega}\psi(x) \tag{2.17}$$

We will rename the variables x and E by the following expressions:

$$\xi = \sqrt{\frac{m\omega}{\hbar}}x \quad , \quad \varepsilon = \frac{E}{\hbar\omega}, \tag{2.18}$$

respectively. Using these changes, the Schrödinger equation reads:

$$-\frac{1}{2}\frac{d^2\psi(\xi)}{d\xi^2} + \frac{1}{2}\xi^2\psi(\xi) = \varepsilon\psi(\xi) \tag{2.19}$$

or, equivalently,

$$\frac{d^2\psi(\xi)}{d\xi^2} + (2\varepsilon - \xi^2)\psi(\xi) = 0 \tag{2.20}$$

The asymptotic behaviour of the last equation when $|\xi| \to \infty$ is completely dominated by ξ^2 over 2ε, so it also has to be true that

$$\frac{d^2\psi(\xi)}{d\xi^2} - \xi^2\psi(\xi) = 0 \tag{2.21}$$

The previous equation has a solution that is a linear combination such that $\psi(\xi) = Ae^{-\xi^2/2} + Be^{+\xi^2/2}$. However, as noted in [10], the B term diverges, rendering it not normalizable and leading to a physically unacceptable solution. So it must be $B = 0$ and, hence, the solution must have the following form:

$$\psi(\xi) = H(\xi)e^{-\xi^2/2} \tag{2.22}$$

Substituting this expression in equation (2.20) we get what is known as Hermite's equation:

$$\frac{d^2H}{d\xi^2} - 2\xi\frac{dH}{d\xi} + (2\varepsilon - 1)H = 0 \tag{2.23}$$

As in [10], we propose that the solution to equation (2.23) is in the form of a power series in ξ:

$$H(\xi) = \sum_{k=0}^{\infty} c_k\xi^k \tag{2.24}$$

Substituting the corresponding terms in equation (2.23), we get

$$\begin{aligned}\sum_{k=0}^{\infty}(k-1)kc_k\xi^{k-2} - \sum_{k=0}^{\infty}2k\xi c_k\xi^{k-1} + (2\varepsilon-1)\sum_{k=0}^{\infty}c_k\xi^k = \\ = \sum_{k=0}^{\infty}(k-1)kc_k\xi^{k-2} + (2\varepsilon - 1 - 2k)\sum_{k=0}^{\infty}c_k\xi^k \\ = \sum_{k=0}^{\infty}\left[(k+1)(k+2)c_{k+2} + (2\varepsilon-1-2k)c_k\right]\xi^k = 0\end{aligned} \tag{2.25}$$

Following [10], from the uniqueness of power series expansions, the coefficients of ξ must be null for all k. Hence, we get the following recursion formula:

$$c_{k+2} = \frac{2k+1-2\varepsilon}{(k+1)(k+2)}c_k \tag{2.26}$$

When k tends to infinity, $\frac{c_{k+2}}{c_k}$ behaves similarly to $\frac{2}{k}$ which has $c_k = \frac{C}{k/2)!}$ as solution, with C as a constant. Adding over all values of k, we get a solution of the form $H(\xi) \sim Ce^{\xi^2}$, which in turn will give $\psi(\xi) \sim Ce^{\xi^2/2}$. However, as said before, the asymptotic behaviour of this solution is not physically possible; therefore, there has to occur a maximum value for k, say n, and $H(\xi)$ has to be a

polynomial. To find this value, we equate $c_{n+2} = 0$ which is equivalent to making the numerator of the recursion formula zero, to get:

$$2n + 1 = 2\varepsilon, \quad n = 0, 1, 2, \ldots$$

Replacing ε by its expression in equation (2.18) we arrive to the condition of the quantization of energy:

$$E_n = \left(n + \frac{1}{2}\right)\hbar\omega, \quad n = 0, 1, 2, \ldots \tag{2.27}$$

As mentioned previously, $H(\xi)$ are polynomials of degree n in ξ, called **Hermite polynomials**. Given that the potential of the harmonic oscillator has even parity, the solutions associated to equation (2.23) will also have a defined parity. Therefore, $H(\xi)$ will contain only even powers if n is even and odd powers if n is odd.

Finally, gathering together all of our results and undoing the variable changes, we get that the solutions of the Schrödinger equation for the one-dimensional harmonic oscillator are of the form:

$$\psi_n(x) = C_n \exp\left(-\frac{m\omega}{2\hbar}x^2\right) H_n\left(\sqrt{\frac{m\omega}{\hbar}}x\right) \tag{2.28}$$

The constant C_n is obtained imposing the normalization condition, that is,

$$1 = \int_{-\infty}^{\infty} |\psi_n(x)|^2 dx = C_n^2 2^n n! \sqrt{\frac{\pi\hbar}{m\omega}} \quad \Rightarrow \quad C_n = \frac{1}{\sqrt{2^n n!}}\left(\frac{m\omega}{\pi\hbar}\right)^{1/4} \tag{2.29}$$

Figure 2.1 shows the first four stationary states for the harmonic oscillator. It can be observed that there is a fundamental state whose associated energy is $E_0 = \frac{1}{2}\hbar\omega$ which is different from zero.

Numerical solution

After solving the Schrödinger equation analytically, we will solve it numerically through diagonalization and using the finite-differences method. We start from the time-independent Schrödinger equation[2]:

$$-\frac{1}{2}\frac{d^2\psi(x)}{dx^2} + V(x)\psi(x) = E\psi(x) \tag{2.30}$$

[2]We will use throughout this discussion the convention that $\hbar = m = \omega = 1$ in the numerical resolution

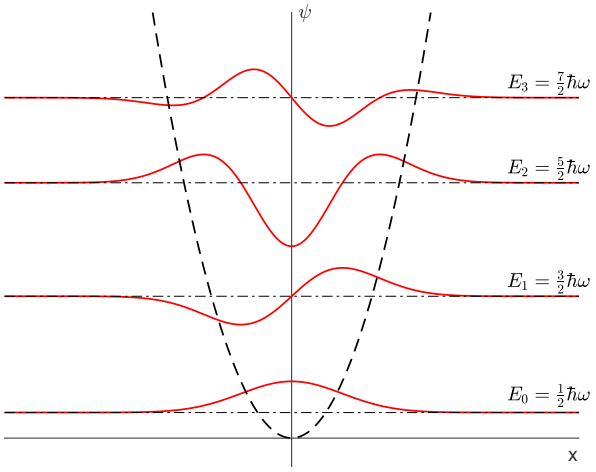

Figure 2.1: First four energy states for the 1D harmonic oscillator. The dashed black line corresponds to the harmonic oscillator potential.

To solve it numerically, we discretise the problem defining the spatial coordinate as an equidistant discrete set of points with spacing $\Delta x = \frac{2L}{N-1}$; hence, we get a mesh from $-L$ to L that has N intervals and $N+1$ points. For each of the discrete values, we denote the solutions by $f_i = f_i(x_i) = \psi(x_i)$.

As noted in [4], the finite difference method expands the function f as a Taylor series around every point of the mesh grid. The value of the function at the neighbouring points of x_i is written as:

$$\begin{aligned} f(x_{i-1}) &= f(x_i) - \Delta x f^{'}(x_i) + \frac{\Delta x^2}{2} f^{''}(x_i) + \mathcal{O}(\Delta x^3) \\ f(x_i) &= f(x_i) \\ f(x_{i+1}) &= f(x_i) + \Delta x f^{'}(x_i) + \frac{\Delta x^2}{2} f^{''}(x_i) + \mathcal{O}(\Delta x^3) \end{aligned} \tag{2.31}$$

Using the first and third expressions, we get the first derivative at x_i

$$f^{'}(x_i) = \frac{f(x_{i+1}) - f(x_{i-1})}{2\Delta x} + \mathcal{O}(\Delta x^2) \tag{2.32}$$

And, finally, in order to approximate the second derivative of f needed in our problem, we use equation (2.32) to get

$$\frac{d^2 f_i}{dx_i^2} = \frac{f_{i+1} - 2f_i + f_{i-1}}{\Delta x^2} \tag{2.33}$$

Substituting this expression in equation (2.30), we get

$$\begin{aligned} -\frac{1}{2}\frac{d^2 f_i}{dx_i^2} + V_i f_i &= E_i f_i \\ \Rightarrow -\frac{1}{2\Delta x^2}\left(f_{i+1} - 2f_i + f_{i-1}\right) + V_i f_i &= E_i f_i \end{aligned} \tag{2.34}$$

We obtain a tridiagonal matrix and, then we generate the Hamiltonian in matrix form, so the problem to be resolved numerically becomes

$$\begin{pmatrix} \frac{1}{\Delta x^2}+V_1 & -\frac{1}{2\Delta x^2} & 0 & \dots & \dots & 0 \\ -\frac{1}{2\Delta x^2} & \frac{1}{\Delta x^2}+V_2 & -\frac{1}{2\Delta x^2} & \dots & \dots & \vdots \\ 0 & -\frac{1}{2\Delta x^2} & \frac{1}{\Delta x^2}+V_3 & -\frac{1}{2\Delta x^2} & \dots & \vdots \\ \vdots & \vdots & & & \vdots & \vdots \\ \vdots & \vdots & & & \vdots & -\frac{1}{2\Delta x^2} \\ 0 & \dots & \dots & 0 & -\frac{1}{2\Delta x^2} & \frac{1}{\Delta x^2}+V_N \end{pmatrix} \begin{pmatrix} f_1 \\ f_2 \\ f_3 \\ \vdots \\ \\ \\ \vdots \\ f_N \end{pmatrix} = E \begin{pmatrix} f_1 \\ f_2 \\ f_3 \\ \vdots \\ \\ \\ \vdots \\ f_N \end{pmatrix} \tag{2.35}$$

After implementing the program in MATLAB code with this numerical method, we obtain the eigenvalues and eigenfunctions of the Schrödinger equation for the harmonic oscillator potential. Figure 2.2 shows the first four resulting eigenfunctions.

The numerical resolution of the Schrödinger equation for the harmonic oscillator potential gives eigenfunctions that are in agreement with the expected results. We also found the expected eigenvalues, as shown in Figure 2.3.

2.2 2D harmonic oscillator

The time-independent Schrödinger equation for the harmonic oscillator extended to Cartesian coordinates (x, y) is the following

$$-\frac{\hbar^2}{2m}\left(\frac{\partial^2\psi(x,y)}{\partial x^2} + \frac{\partial^2\psi(x,y)}{\partial y^2}\right) + V(x,y)\psi(x,y) = E\psi(x,y) \tag{2.36}$$

where the harmonic oscillator potential takes now the form

$$V(x,y) = \frac{1}{2}k(x^2+y^2), \tag{2.37}$$

and is shown in Figure 2.4.

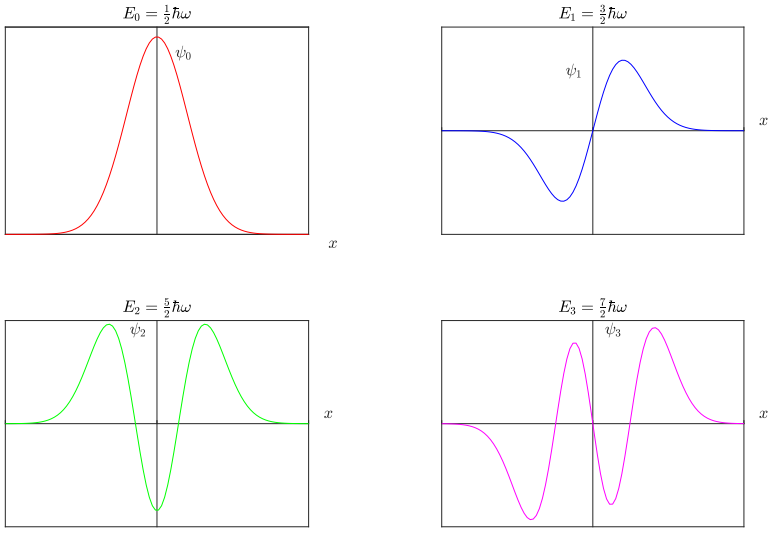

Figure 2.2: First four eigenfunctions for the harmonic oscillator by numerical method.

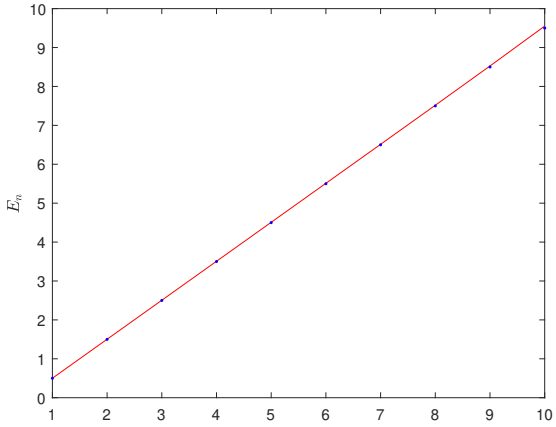

Figure 2.3: Ten first eigenvalues obtained numerically against the analytical solution $E = n + 1/2$ in red.

We use separation of variables to solve the equation, that is, we assume solutions take the form $\psi(x, y) = X(x)Y(y)$. Substituting this expression in equation (2.36), we get

$$-\frac{\hbar^2}{2m}\left(Y\frac{\partial^2 X}{\partial x^2} + X\frac{\partial^2 Y}{\partial y^2}\right) + V(x,y)XY = EXY \tag{2.38}$$

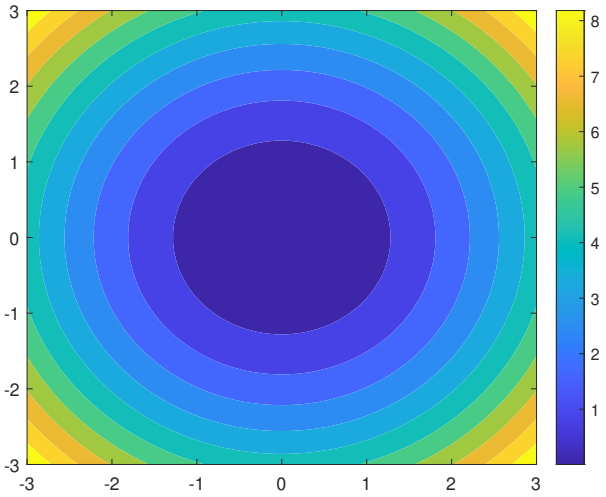

Figure 2.4: Two-dimensional harmonic oscillator potential.

Next, dividing by XY:

$$\left(-\frac{1}{X}\frac{\hbar^2}{2m}\frac{\partial^2 X}{\partial x^2}+\frac{1}{2}kx^2\right)+\left(-\frac{1}{Y}\frac{\hbar^2}{2m}\frac{\partial^2 Y}{\partial y^2}+\frac{1}{2}ky^2\right)=E \tag{2.39}$$

We observe that the Hamiltonian of the two-dimensional system can be separated into two one-dimensional harmonic oscillator Hamiltonians $\hat{H}=\hat{H}_x+\hat{H}_y$ whose sum equals a constant; hence, suggesting that each term must be a constant, which we will denote with E_x and E_y

$$\begin{aligned}\left(-\frac{\hbar^2}{2m}\frac{\partial^2}{\partial x^2}+\frac{1}{2}kx^2\right)X(x)&=E_xX\\ \left(-\frac{\hbar^2}{2m}\frac{\partial^2}{\partial y^2}+\frac{1}{2}ky^2\right)Y(y)&=E_yY\end{aligned} \tag{2.40}$$

such that $E_x+E_y=E$.

In the previous section we have already solved the one-dimensional harmonic oscillator problem; therefore, by analogy the energy states are

$$E_x=\left(n_x+\frac{1}{2}\right)\hbar\omega \quad , \quad E_y=\left(n_y+\frac{1}{2}\right)\hbar\omega \quad , \; n_x,n_y=0,1,2,\ldots \tag{2.41}$$

and the same happens for the eigenfunctions:

$$\begin{aligned} X_{n_x}(x) &= \frac{1}{\sqrt{2^{n_x} n_x!}} \left(\frac{m\omega}{\pi\hbar}\right)^{1/4} \exp\left(-\frac{m\omega}{2\hbar}x^2\right) H_{n_x}\left(\sqrt{\frac{m\omega}{\hbar}}x\right) \\ Y_{n_y}(y) &= \frac{1}{\sqrt{2^{n_y} n_y!}} \left(\frac{m\omega}{\pi\hbar}\right)^{1/4} \exp\left(-\frac{m\omega}{2\hbar}y^2\right) H_{n_y}\left(\sqrt{\frac{m\omega}{\hbar}}y\right) \end{aligned} \tag{2.42}$$

Consequently, the general analytical solution for eigenfunctions and eigenvalues of the two-dimensional harmonic oscillator Schrödinger equation can be written as follows

$$\psi(x,y) = \frac{1}{\sqrt{2^{n_x+n_y} n_x! n_y!}} \sqrt{\frac{m\omega}{\pi\hbar}} \exp\left(-\frac{m\omega}{2\hbar}(x^2+y^2)\right) H_{n_x}\left(\sqrt{\frac{m\omega}{\hbar}}x\right) H_{n_y}\left(\sqrt{\frac{m\omega}{\hbar}}y\right)$$

$$E = (1 + n_x + n_y)\hbar\omega = (1+n)\hbar\omega \quad , \quad n_x, n_y = 0, 1, 2, \ldots \tag{2.43}$$

As we can see from the analytical solutions the energy states of the harmonic oscillator are degenerate, with a degeneracy equal to $n+1$. This is shown in Figure 2.5 where we have plotted the probability density $|\psi(x,y)|^2$. The fundamental state $(0,0)$, that corresponds to energy $E_0 = \hbar\omega$, has no degeneracy; however, the energy state $E_1 = 2\hbar\omega$ has a degeneracy of 2, $(1,0)$ and $(0,1)$. The second row shows the degeneracy of 3 for the energy state $E_2 = 3\hbar\omega$: $(1,1)$, $(2,0)$ and $(0,2)$. And so on.

Numerical solution

The two-dimensional harmonic oscillator problem is analogous to the previous one, we start from the two-dimensional time-independent Schrödinger equation:

$$-\frac{1}{2}\left(\frac{\partial^2}{\partial x^2} + \frac{\partial^2}{\partial y^2}\right)\psi(x,y) + V(x,y)\psi(x,y) = E\psi(x,y) \tag{2.44}$$

Now the solutions are discretised over a grid of N^2 points with $\Delta x = \frac{2L}{N-1}$ and $\Delta y = \frac{2L}{N-1}$ as the lattice spacing for each of the Cartesian coordinates. The solution eigenfunctions will be denoted by $f_{i,j} = \psi_{i,j}$ for $i, j = 1, \ldots, N$. Therefore, the state representation of wave functions will now be a matrix of size $N \times N$ which will take the form:

$$\begin{pmatrix} f_{1,1} & f_{1,2} & \cdots & \cdots & f_{1,N} \\ f_{2,1} & f_{2,2} & \cdots & \cdots & f_{2,N} \\ \vdots & \vdots & & \ddots & \vdots \\ f_{N,1} & f_{N,2} & \cdots & \cdots & f_{N,N} \end{pmatrix} \tag{2.45}$$

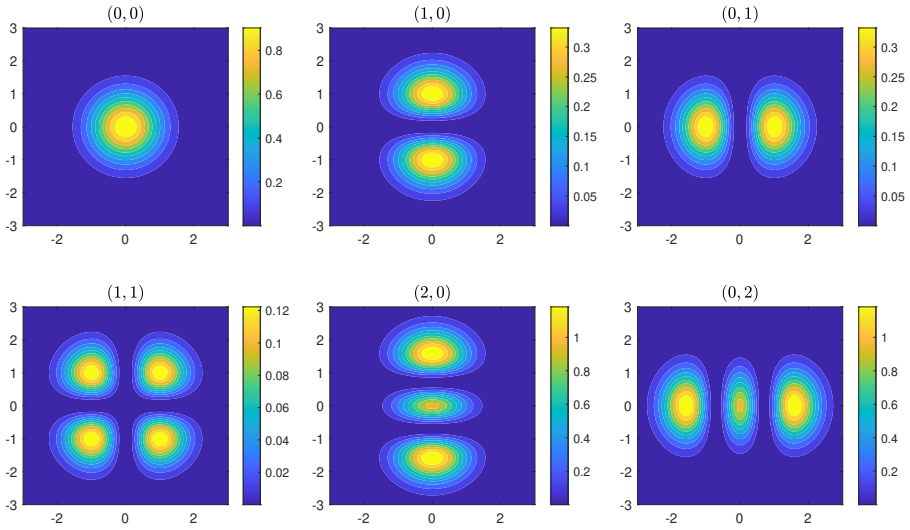

Figure 2.5: Two-dimensional harmonic oscillator probability densities $|\psi(x,y)|^2$ for states (n_x, n_y) obtained analytically.

However, to be read by MATLAB we will arrange it in the form of a N^2 vector:

$$\begin{pmatrix} f_{1,1} \\ \vdots \\ f_{1,N} \\ \vdots \\ f_{N,1} \\ \vdots \\ f_{N,N} \end{pmatrix}$$

As with the one-dimensional harmonic oscillator, we use the finite-difference method to approximate the Laplacian and, hence, we will use the analogue to equation (2.33) in the (x,y) plane:

$$\frac{\partial f_{i,j}}{\partial x^2} = \frac{f_{i+1,j} - 2f_{i,j} + f_{i-1,j}}{\Delta x^2} \quad , \quad \frac{\partial^2 f_{i,j}}{\partial y^2} = \frac{f_{i,j+1} - 2f_{i,j} + f_{i,j-1}}{\Delta y^2} \tag{2.46}$$

Applying this approximation and taking the same spacing step in both coordinates, $\Delta x = \Delta y \equiv \Delta$, equation (2.44) becomes

$$-\frac{1}{2}\left(\frac{f_{i+1,j} - 2f_{i,j} + f_{i-1,j}}{\Delta^2} + \frac{f_{i,j+1} - 2f_{i,j} + f_{i,j-1}}{\Delta^2}\right) + V_{i,j} f_{i,j} = E f_{i,j} \tag{2.47}$$

Arranging terms we get:

$$-\frac{1}{2\Delta^2}\left(f_{i+1,j}+f_{i-1,j}-4f_{i,j}+f_{i,j+1}+f_{i,j-1}\right)+V_{i,j}f_{i,j}=Ef_{i,j} \tag{2.48}$$

Finally, the problem to be solved numerically in matrix notation becomes:

$$\frac{1}{\Delta^2}\begin{pmatrix} 2+V_{1,1} & -1/2 & 0 & -1/2 & 0 & 0 & \dots & \dots & 0 \\ -1/2 & 2+V_{1,2} & -1/2 & 0 & -1/2 & 0 & \dots & \dots & 0 \\ 0 & -1/2 & 2+V_{1,3} & 0 & 0 & -1/2 & 0 & \dots & 0 \\ \vdots & \vdots & \vdots & & & \ddots & \ddots & & 0 \\ \vdots & \vdots & \vdots & & & & \ddots & \ddots & 0 \\ 0 & 0 & \dots & \dots & -1/2 & 0 & -1/2 & 2+V_{N,N-1} & -1/2 \\ 0 & 0 & \dots & \dots & \dots & -1/2 & 0 & -1/2 & 2+V_{N,N} \end{pmatrix}\begin{pmatrix} f_{1,1} \\ f_{1,2} \\ \vdots \\ f_{1,N} \\ \vdots \\ f_{N,1} \\ \vdots \\ f_{N,N} \end{pmatrix} = E\begin{pmatrix} f_{1,1} \\ f_{1,2} \\ \vdots \\ f_{1,N} \\ \vdots \\ f_{N,1} \\ \vdots \\ f_{N,N} \end{pmatrix} \tag{2.49}$$

To obtain the eigenvalues and eigenfunctions, we first create a sparse $N \times N$ matrix L of the form:

$$L=\frac{1}{\Delta^2}\begin{pmatrix} -2 & 1 & 0 & \dots & \dots & 0 \\ 1 & -2 & 1 & 0 & \dots & 0 \\ 0 & 1 & -2 & 1 & \dots & 0 \\ \vdots & \vdots & & \ddots & & \vdots \\ \vdots & \vdots & & & \ddots & 0 \\ 0 & 0 & \dots & 1 & -2 & 1 \\ 0 & 0 & \dots & 0 & 1 & -2 \end{pmatrix} \tag{2.50}$$

We calculate the $N^2 \times N^2$ matrix representing the two-dimensional Laplacian $L2$ as the sum of two sparse matrices which are obtained as the Kronecker tensor product of L and I, where I is the identity matrix. That is,

$$L2 = L \otimes I + I \otimes L \tag{2.51}$$

After constructing a sparse $N^2 \times N^2$ matrix for the harmonic oscillator potential

$$V=\begin{pmatrix} V_{1,1} & 0 & \dots & \dots & 0 \\ 0 & V_{1,2} & 0 & \dots & 0 \\ \vdots & \vdots & \vdots & \dots & 0 \\ 0 & 0 & \dots & \dots & V_{N,N} \end{pmatrix},$$

we finally obtain the two-dimensional Hamiltonian as:

$$H=-\frac{1}{2}L2+V \tag{2.52}$$

We diagonalize the resulting matrix for the Hamiltonian to obtain the eigenvalues and eigenfunctions. Figure 2.6 shows the probability densities obtained from

numerically solving the two-dimensional Schrödinger equation for the harmonic oscillator potential. The numerical results are in agreement with the theoretical wave functions and accurately capture their characteristics.

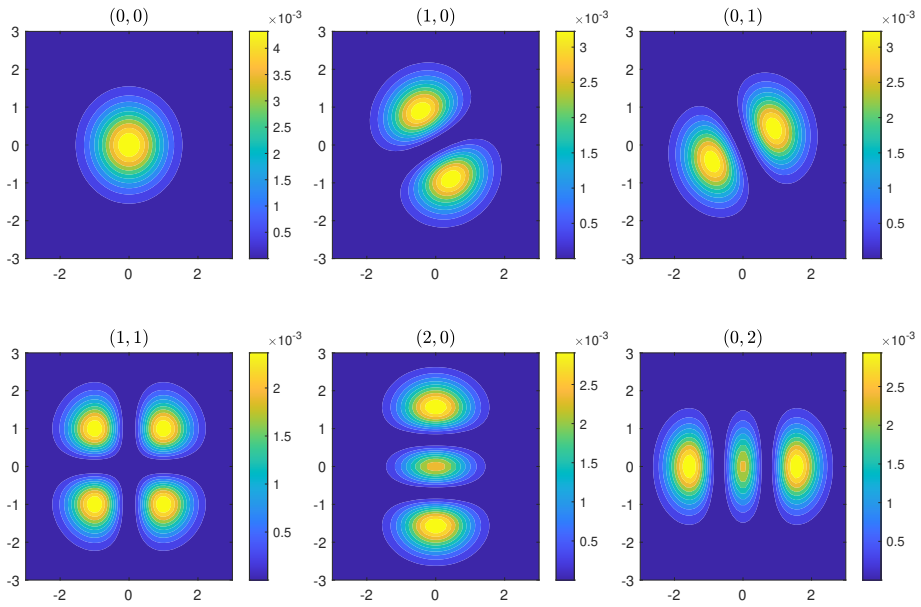

Figure 2.6: Two-dimensional harmonic oscillator probability densities $|\psi(x,y)|^2$ for states (n_x, n_y) obtained numerically.

Chapter 3

Quantum scars

Determinism is at the essence of classical mechanics, it establishes that, given the precise initial conditions of a particular system, Newton's laws govern its motion evolution through a set of ordinary differential equations and, hence, the future state of the system can be predicted. It is also possible to prove that the solutions to Newton's equations exist and are unique, hence providing a "'clockwork"' understanding of the future evolution of the system.

In practice, however, determinism is not guaranteed, except maybe for the simplest of systems. Albeit the motion of a system can be strictly calculated, the presence of chaos makes it highly sensitive to the surrounding conditions, subsequently making it impossible to produce accurate predictions. We would need to know with infinite accuracy the conditions of the system to be able to trace its evolution.

In the previous chapter, we have solved the Schrödinger equation and have obtained as a solution a wave function $\psi(\vec{r}, t)$ which, when squared, gives us the likelihood $|\psi(\vec{r}, t)|^2$ of finding our particle at a certain location at a certain moment in time. This stems from Born's statistical interpretation of the wave function and, with it, introduces the indeterminism in quantum mechanics. Consequently, one could argue that quantum physics is probabilistic, but not chaotic.

Chaos in the classical world, as described in the first chapter, arises when a system is highly sensitive to its initial conditions so that a small perturbation alters its future behaviour in an exponentially growing manner. In contrast, chaos should not exist in the quantum world since small perturbations generally lead to small changes in future states. At this point, one could wonder how chaos can exist in the world when macroscopic systems are ultimately made out of atoms

which are quantum in essence, why does not quantum regularity triumph on the larger scale? There are two confronting answers to this question. Some argue that the quantum break time −the time-scale after which quantum mechanics diverges from the classical evolution and chaos can no longer be suppressed by quantum regularity− gets longer and longer. Others, as Berry in [1], find that the dominance of chaos comes from the inability of isolating large quantum systems from their surrounding universe.

A quantum system is undetermined in the sense that the Heisenberg uncertainty principle establishes, namely, that we cannot know at the same time and with total precision the position and momentum of our particle when measuring them. This uncertainty is quantized by Planck's constant $\hbar$. Therefore, we can only predict the probabilities of the different known outcomes. In quantum mechanics, the indeterminism does not come from the Schrödinger equation, but from the act of measuring.

The probabilistic interpretation is one of the most notable differences between classical and quantum mechanics. Furthermore, unlike its counterpart, classical mechanics is able to measure simultaneously all its observables, delivering trajectories that may be distinguishable from one another. Classical physics also has the observer of the system play a passive role, whereas in quantum mechanics the observer is a source of disturbance whose effects on the system under analysis are not trivial.

The question of what quantum chaos is still prompts a debate. However, attempts have been made to answer some of the questions that the presence of chaos raises, such as how chaos moves from the classical scale to the smooth quantum world, how the two distinct worlds can be reconciled or whether even chaos exists in the quantum world. As Bohr correspondence principle is the bridge that connects quantum and classical mechanics in the sense that the behaviour description of a system made by quantum theory recovers, in the limit of large quantum numbers, the classical characterization; quantum chaos is the link between classical chaotic systems and quantum physics.

It is largely accepted that, as mentioned in [5], there are three different types of quantum chaos: "'quantized chaos"', "'semiquantum chaos"' and proper "'quantum chaos"'. The first type of quantum chaos has been the most studied one and it concerns the quantization of classically chaotic systems in the semiclassical limit ($\hbar \to 0$). Semiquantum chaos studies quantum-classical coupled systems such as

the ones that can be found in molecular physics or billiards that have vibrating boundaries. Lastly, the "'true"' quantum chaos deals with fully quantized systems that show an exponential sensitive dependence on initial conditions. In this chapter, we will focus on the first type, quantized chaos, also referred to as "'quantum chaology"'.

Quantized chaos looks for trademarks of classically chaotic systems on the quantum level. A large number of systems such as atoms in excited high-energy states or the double pendulum, to name a few of the simplest ones, manifest chaotic properties when analysed through the classical lens. Although the quantized system does not exhibit sensitivity to small changes in the initial conditions, the underlying chaos bleeds to the quantum level where the corresponding wave functions and energies get strongly influenced by it. Actually, this has been one of the most surprising discoveries, the fact that quantum systems feel whether their classical counterparts display a chaotic behaviour or not: chaos in the classical system manifests itself in the associated quantum dynamics that, albeit not chaotic, "'register"' the chaos manifested in the macro-scale.

Usually, the study of quantum chaos starts with a classically chaotic system which is not isolated from its surrounding environment and where the quantum regularity is not present. Then, the system gets quantized (a challenging process and not straightforward whatsoever) and analysed in the semiclassical limit so as to identify its classical chaotic characteristics. These quantum systems manifest classical chaos in several ways, as for instance, quantum "'scars"'.

The term quantum "'scars"' was first coined by Heller in his paper [13] where he examined the effects of unstable periodic orbits on the eigenfunctions of the classically chaotic stadium billiard. From a classical viewpoint and as mentioned in [11], a conventional trajectory in the stadium billiard evenly covers the stadium space, suggesting that the stationary states might look random. Nonetheless, Heller's work found that, at the quantum level, unstable, periodic orbits induced an enhancement along their trajectories in the sense that a larger than expected density surrounded some of these wave functions. As [11] points out, these orbits that do not stand out in the classical world become predominant in the quantum scale.

Let's go back to the Bunimovich stadium since this has been one of the simplest and most used billiards to study quantum chaos. From the classical perspective, the particle inside the Bunimovich stadium evolves following the billiard ball map

in equation (1.9), while the quantum evolution is described by the Schrödinger equation. Following [19], the Laplacian of this problem has a countable sequence of eigenfunctions $\psi_1, \psi_2, \ldots$ associated to an increasing sequence of eigenvalues $E_1, E_2, \ldots$ which are normalised so that $\int_{billiard} |\psi_k|^2 = 1, \forall k$. The conjecture associated with this problem in the physical space reads as follows:

Conjecture 3.1. ***Scarring conjecture.*** *There exists a subset $A \subset \Omega$ and a sequence ψ_{k_j} of eigenfunctions with $E_{k_j} \to \infty$ such that $\int_A |\psi_{k_j}|^2$ does not converge to $|A|/|\Omega|$. That is, the eigenfunctions "'scar"' in A or on the complement of A.*

In the Bunimovich stadium, the set A corresponds to the union of all vertical trajectories in which the billiard bounces orthogonally off the flat edges of the stadium infinitely. This conjecture establishes that the eigenfunctions f_k are not equally distributed in the physical space when $k \to \infty$, that is, the quantum unique ergodicity fails as the energy becomes larger.

Closely following the numerical method use in the two-dimensional harmonic oscillator case, we solve the Schrödinger equation so as to obtain the eigenfunctions for the Bunimovich stadium. We consider a rectangle of length $L = 2$ and the semicircles capping it have radius $R = 1$, thus obtaining a mesh-grid of points such that $-(L/2 + R) \leq x \leq L/2 + R$ and $-R \leq y \leq R$. With these characteristics, the minimal energy obtained is approximately $E_0 \sim \frac{\hbar^2}{mL^2} \sim \frac{1}{L^2}$, therefore, we choose a potential barrier of $V_0 = 10^3$ so that $V_0 >> E_n, \forall n$.

We arrange all the elements of the array in a $N^2 \times 2$ matrix A where the first column corresponds to values of x and the second column to values of y. Since the potential function in this system is taken to be $V = 0$ if the considered point is inside the billiard and $V = \infty$ if it is on the boundary, we write an indicator function to help us find these points. The function *ind* is built to satisfy the following conditions with a tolerance $tol = 10^{-4}$

- $(x - L/2)^2 + y^2 > R^2$ and $x > L/2 - tol$
- $(x + L/2)^2 + y^2 > R^2$ and $x < -L/2 + tol$
- $|y^2 - R| < tol$
- $|y^2 + R| < tol$

and reports those points in A that satisfy them. These points have an assigned potential of $V = V_0$ in the corresponding potential matrix V.

Using the lattice spacing for each coordinate Δx and Δy, we write two sparse tridiagonal matrices that correspond to the 1D finite difference Laplacians, $LapX$ and $LapY$, equally to what was done in the previous section in matrix (2.50). We again calculate the $N^2 \times N^2$ matrix representing the two-dimensional Laplacian $L2$ as the sum of two sparse matrices which are obtained as the Kronecker tensor product of $LapX/LapY$ and I, where I is the identity matrix. That is,

$$L2 = LapX \otimes I + I \otimes LapY \tag{3.1}$$

Finally, the two-dimensional Hamiltonian for the Bunimovich stadium billiard is

$$H = -\frac{1}{2}L2 + V \tag{3.2}$$

Figure 3.1 presents the familiar diagrams for the density functions, similar to the ones we have obtained for the case of the two-dimensional harmonic oscillator.

The following figure 3.2 shows the presence of quantum "'scars"' on the Bunimovich stadium, when starting from a higher energy value $n = 81$, since it is from larger quantum numbers that the classical chaos starts to become apparent at the quantum level. Some of the scars in this diagram are associated to unstable periodic orbits that leave their imprint on the quantum world.

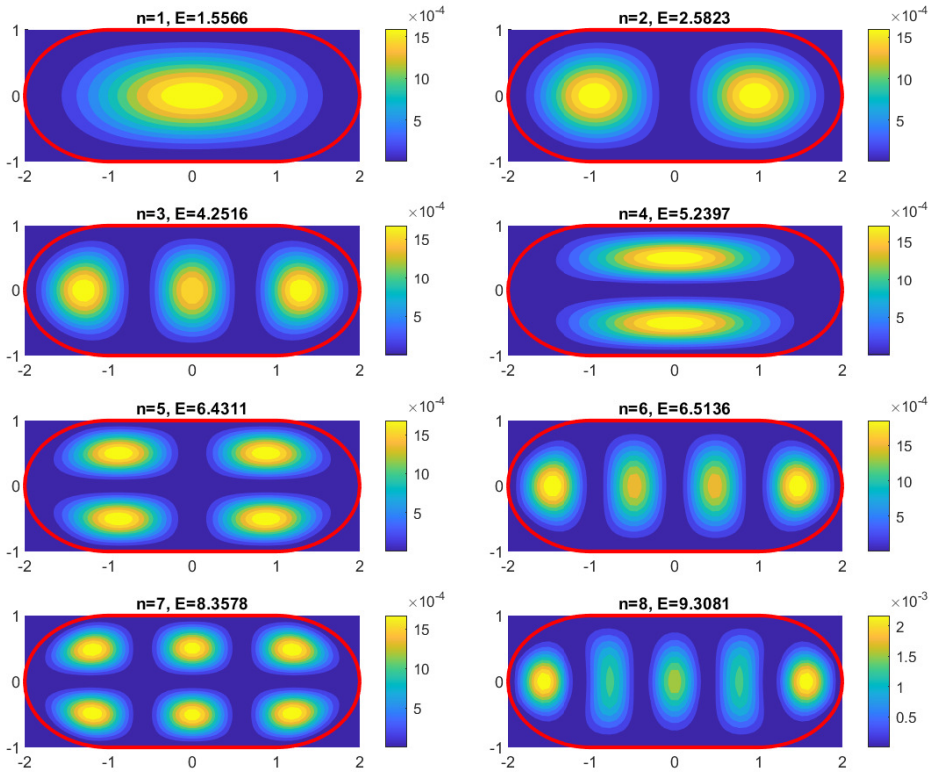

Figure 3.1: Probability densities in the Bunimovich stadium associated with the first eight eigenvalues.

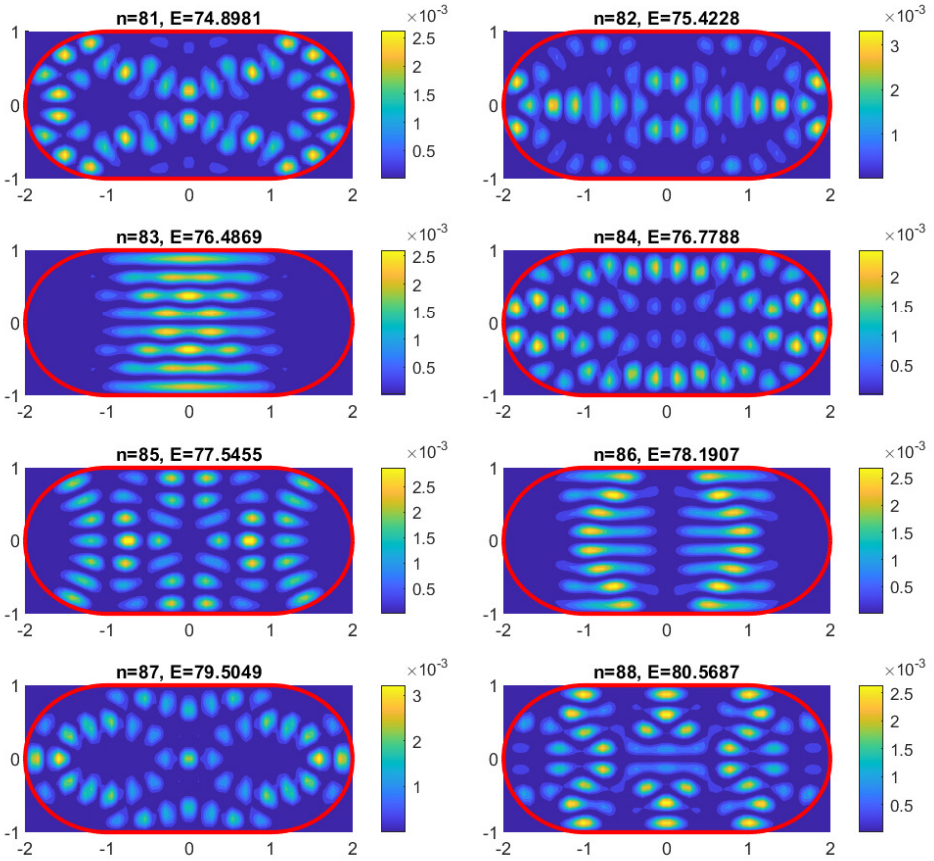

Figure 3.2: Consecutive density functions in the Bunimovich stadium, starting at $E = 74.9$.

Conclusions

In this work we have studied, in the first place, billiards as dynamical systems that have such a versatile character that are able to model very different situations. As we have shown, one of the most important features of a billiard is its boundary, given that its geometry strongly influences the dynamics of the particle within. We started our study with circular and square billiard tables which display a regular behaviour, and later introduced the ones that interest us which are able to generate completely chaotic patterns.

In this light, we have presented a particularly special type of billiard, the Bunimovich stadium. This billiard is famously chaotic since the trajectories of a billiard in motion inside its domain are highly difficult to predict: given two marginally different initial conditions, the trajectories followed by the two billiards differ exponentially as time goes by. Another important result is its ergodicity which Bunimovich proved in [6], hence, we know that the position of a billiard with a given initial position and velocity will uniformly and randomly be distributed over the whole stadium.

In Chapter 2, we have also explored the Schrödinger equation. We have introduced the steps for its resolution in the case of conservative physical systems, that is, where the potential does not depend on time. In the special case of the simple harmonic oscillator potential, we have studied the analytical solution for the one and two-dimensional cases in Cartesian coordinates. Additionally, we have also used a finite-differences method to obtain a numerical solution to the Schrödinger equation. In doing so, we have found that the probability densities obtained from the numerical analysis are in completely agreement with the theoretical ones as can be observed in the corresponding Figures 2.1 and 2.2 for the one-dimensional case and Figures 2.5 and 2.6 for the two-dimensional.

Finally, in Chapter 3, we have ventured inside quantum chaotic billiards by solving the Schrödinger equation numerically for the Bunimovich stadium. Our

results are able to replicate quantum "'scars"' in this billiard, a term coined by Heller in [13] and that has no analogue in the classical framework. As shown in Figure 3.2, the density functions associated to classical unstable periodic orbits manifest as enhanced probability density regions around their classical trajectories.

Since this work touches upon a very active research field, there are still areas to improve and to expand upon in possible future research. On one hand, it would be important to translate the numerical analysis from the MATLAB programming to a C language or similar and develop optimal methods to find eigenvalues and eigenvectors of huge sparse matrices which we obtain at discretization of the Schrödinger equation. On the other hand, there is still more to contribute in the area of chaotic dynamics, a possible extension of this work would include an analysis of the quantum behaviour in other known chaotic billiards such as mushroom billiards and heart or lemon-shaped billiards.

Bibliography

[1] Al-Khalili, J., *Quantum: a guide for the perplexed*, Weidenfeld Nicolson, 2003.

[2] Bäcker, A., *Quantum chaos in billiards*, Institut für Theoretische Physik.

[3] Baez, J., *Bunimovich Stadium*, American Mathematical Society Blogs, 2016.

[4] Becerril, R. et al, *Solving the time-dependent Schrödinger equation using finite difference methods*, Revista Mexicana de Física E, **54**(2), 120-132.

[5] Blümel, R. et al, *Chaos in Atomic Physics*, Cambridge University Press, 1997.

[6] Bunimovich, L., *On ergodic properties of nowhere dispersing billiards*, Commun. Math. Phys. **65**, 1979.

[7] Bunimovich, L., *Dynamical billiards*, Scholarpedia, **2(8)**:1813 (2007).

[8] Chernov, N. and Markarian, R., *Chaotic billiards*, Mathematical surveys and monographs **127**, American Mathematical Society (2006).

[9] Devaney, R.L., *A First Course in Chaotic Dynamical Systems: Theory and Experiment*, Studies in Nonlinearity, Avalon Publishing, 1992.

[10] Griffiths, D., *Introduction to Quantum Mechanics*, Pearson Prentice Hall, New Jersey, 2005.

[11] Gutzwiller, M.C., *Chaos in Classical and Quantum Mechanics*, Interdisciplinary Applied Mathematics Volume 1, Springer, 1990.

[12] Harris, G., *Polygonal Billiards*, Southern Illinois University Edwardsville (2007).

[13] Heller, E.J., *Bound-State Eigenfunctions of Classically Chaotic Hamiltonian Systems: Scars of Periodic Orbits*, Phys. Rev. Lett., **53**, Number 16, 1984.

[14] Heller, E.J. et al *The Eigenfunctions of Classically Chaotic Systems*, Phys. Scr. **40**, 354, 1989.

[15] Porter, M.A., *An Introduction to Quantum Chaos*, Centre for Applied Mathematics, Cornell University,2001.

[16] Shoemaker, R., *Modeling a chaotic billiard: The Bunimovich Stadium*, James Madison University, JMU Scholarly Commons, 2019.

[17] Sinai, Y., *Kolmogorov-Sinai entropy*, Scholarpedia, **4(3)**:2034.

[18] Tabachnikov, S., *Geometry and Billiards*, American Mathematical Society (2005).

[19] Tao, T., <https://terrytao.wordpress.com/2008/07/07/hassells-proof-of-scarring-for-the-bunimovich-stadium>, accessed 10 May 2022.

[20] Yeung, E., *Quantum Chaos in a Billiard System*, University of Toronto, 2013.

Appendix

Code for solving the 2D Schrödinger equation with simple harmonic oscillator potential

```
clear all
L=3;
g = 50; g2 = g^2;
p = linspace(-L, L, g);          % one dimensiton space
    lattice
[X, Y] = meshgrid(p, p);  % two dimension space lattice
h = p(2) - p(1);                 % latice spacing
X = X(:); Y = Y(:);   % all elements of arraty as a single
    column
R = 0.5*(X.^2 + Y.^2);   % distance from the center
Vext = R;                  % potential energy
e = ones(g,1);
L = spdiags([e -2*e e], -1:1, g, g) / h^2; % 1D finite
    difference Laplacian
I = speye(g);
L2 = kron(L,I) + kron(I, L);  % extend Laplacian to 2 D
H = -0.5 * L2 + spdiags(Vext, 0, g2, g2);  % Hamiltonian of
    H atom
[PSI,E] = eigs(H, 10, 'sa');          % Smallest eigenvalues
    of H
i=1;
X1=reshape(X,g,g);
Y1=reshape(Y,g,g);
PSI1=reshape(PSI(:,i),g,g);
contourf(X1,Y1,PSI1, 10, 'LineStyle','none');
colorbar % shows the bar with the color scale
```

Code for solving the 2D Schrödinger equation in the Bunimovich stadium

```
clear all;
L=2; R=1; V0=1000; tol=1e-4;
g = 50; g2 = g^2;
px = linspace(-(L/2+R), (L/2+R), g);
py = linspace(-R, R, g);          % one dimensiton space
    lattice
[X, Y] = meshgrid(px, py);  % two dimension space lattice
hx = px(2) - px(1)
hy = py(2) - py(1);                  % latice spacing
A = [X(:), Y(:)];   % all elements of array as two columns

Vext = zeros(g2,1);                   % potential energy
ind=find(((A(:,1)-L/2).^2+A(:,2).^2>R^2)&(A(:,1)>L/2-tol));
ind=[ind; find(((A(:,1)+L/2).^2+A(:,2).^2>R^2)&(A(:,1)<-L/2+
    tol))];
ind=[ind; find(abs(A(:,2)-R)<tol)];
ind=[ind; find(abs(A(:,2)+R)<tol)];
ind=unique(ind);
Vext(ind,:)=V0;

%Discretization of Schrodinger Equation
e = ones(g,1);
LapX = spdiags([e -2*e e], -1:1, g, g) / hx^2; % 1D finite
    difference Laplacian
LapY = spdiags([e -2*e e], -1:1, g, g) / hy^2;
I = speye(g);
L2 = kron(LapX,I) + kron(I, LapY);  % extend Laplacian to 2
    D
H = -0.5 * L2 + spdiags(Vext, 0, g2, g2);  % Hamiltonian of
    H atom
[PSI,E] = eigs(H, 200, 'sa');   % Smallest eigenvalues of H

i=81; E(i,i)

%Represent density of probability of eigenfunction
hold on;
```

```
32 title(['n=', num2str(i), ', E=', num2str(E(i,i))]);
33 PSI2=reshape(PSI(:,i),g,g);
34 Dens=PSI2.*PSI2;
35 contourf(X,Y,Dens, 10, 'LineStyle','none');
36
37 colorbar % shows the bar with the color scale
38
39 %Represent biliard
40 plot([-L/2, L/2], [R, R], 'r', 'LineWidth',3);
41 plot([-L/2, L/2], [-R, -R], 'r', 'LineWidth',3);
42 x1=-L/2-R:0.01:-L/2;
43 y1=sqrt(R^2-(x1+L/2).^2);
44 plot(x1, y1, 'r', 'LineWidth',3);
45 plot(x1,-y1,'r', 'LineWidth',3);
46 plot(-x1, y1, 'r', 'LineWidth',3);
47 plot(-x1,-y1,'r', 'LineWidth',3);
48
49 hold off;
```